

Multipartite entanglement of the topologically ordered state in a perturbed toric code

Yu-Ran Zhang ^{1,2}, Yu Zeng,³ Tao Liu,^{1,4} Heng Fan,^{3,5,*} J. Q. You ^{6,†} and Franco Nori ^{1,2,7,‡}

¹Theoretical Quantum Physics Laboratory, RIKEN Cluster for Pioneering Research, Wako-shi, Saitama 351-0198, Japan

²RIKEN Center for Quantum Computing (RQC), Wako-shi, Saitama 351-0198, Japan

³Institute of Physics, Chinese Academy of Sciences, Beijing 100190, China

⁴School of Physics and Optoelectronics, South China University of Technology, Guangzhou 510640, China

⁵CAS Center for Excellence in Topological Quantum Computation, UCAS, Beijing 100190, China

⁶School of Physics, Zhejiang University, Hangzhou 310027, China

⁷Physics Department, University of Michigan, Ann Arbor, Michigan 48109-1040, USA



(Received 13 September 2021; accepted 12 April 2022; published 24 May 2022)

We demonstrate that multipartite entanglement, witnessed by the quantum Fisher information, can characterize topological quantum phase transitions in the spin- $\frac{1}{2}$ toric code model (TCM) on a square lattice with external fields. We show that the quantum Fisher information density of the ground state can be written in terms of the expectation values of gauge-invariant Wilson loops for different sizes of square regions and identify \mathbb{Z}_2 topological order by its scaling behavior. Furthermore, we use this multipartite entanglement witness to investigate thermalization and disorder-assisted stabilization of topological order after a quantum quench. Moreover, with an upper bound of the quantum Fisher information, we demonstrate the absence of finite-temperature topological order in the two-dimensional TCM in the thermodynamic limit. Our results provide insights to topological phases, which are robust against external disturbances and are candidates for topologically protected quantum computation.

DOI: [10.1103/PhysRevResearch.4.023144](https://doi.org/10.1103/PhysRevResearch.4.023144)

I. INTRODUCTION

Recent developments of quantum information theory have provided novel angles and tools for modern condensed matter physics [1]. The quantum-information features of quantum matter help to study quantum phase transitions (QPTs) [2–7], out-of-equilibrium quantum many-body systems [8–10], and non-Hermitian physics [11–16]. One pivotal concept introduced by quantum information science into condensed matter physics is quantum entanglement [17], which quantifies *nonlocal* quantum correlations. Beyond Landau’s symmetry-breaking theory [3], topological order [18] in strongly correlated many-body systems, e.g., quantum spin liquids [19] and the fractional quantum Hall states [20], can be described by the long-range entanglement encoded in the ground states of the system [1]. Topological order is promising for applications in fault-tolerant quantum computation [21,22] because of properties such as ground-state degeneracy and the non-Abelian geometric phase of degenerate ground states. As a simple example of a stabilizer code, the toric

code model (TCM), with fourfold topological degeneracy on a torus, is the widest studied model of topological order, allowing for encoding two robust qubits against *local* perturbations [21].

Bipartite entanglement witnesses, including topological entanglement entropy [23,24], entanglement spectrum [25], topological Rényi entropy [26,27], and entanglement negativity [28,29], have achieved great success in characterizing topological order. However, the measurement of bipartite entanglement requires quantum state tomography or a statistical protocol via randomized measurements [30], which are almost impossible even for a modest system size. Multipartite entanglement, witnessed by the quantum Fisher information (QFI) [31–33], is believed to represent richer properties of complex structures of topological states than bipartite entanglement, which is experimentally measurable in large many-body systems using mature techniques [34–38]. Recent studies [39,40] have shown that the scaling behavior of the QFI with respect to *nonlocal* operators is sensitive when detecting one-dimensional (1D) symmetry-protected topological (SPT) order [41,42] and topological order in the Kitaev honeycomb model [43]. Moreover, the QFI is an effective entanglement witness for a mixed state [33] and is useful for characterizing topological phases at finite temperatures.

In this paper, we demonstrate the characterization of topological QPTs in a two-dimensional (2D) spin- $\frac{1}{2}$ TCM with external fields by using multipartite entanglement, witnessed by the QFI. With a dual transformation [40], the QFI density of the ground state can be expressed in terms of the reduced Wilson loops [44] for different sizes of square regions,

*hfan@iphy.ac.cn.

†jqyou@zju.edu.cn.

‡fnori@riken.jp.

Published by the American Physical Society under the terms of the [Creative Commons Attribution 4.0 International](https://creativecommons.org/licenses/by/4.0/) license. Further distribution of this work must maintain attribution to the author(s) and the published article’s title, journal citation, and DOI.

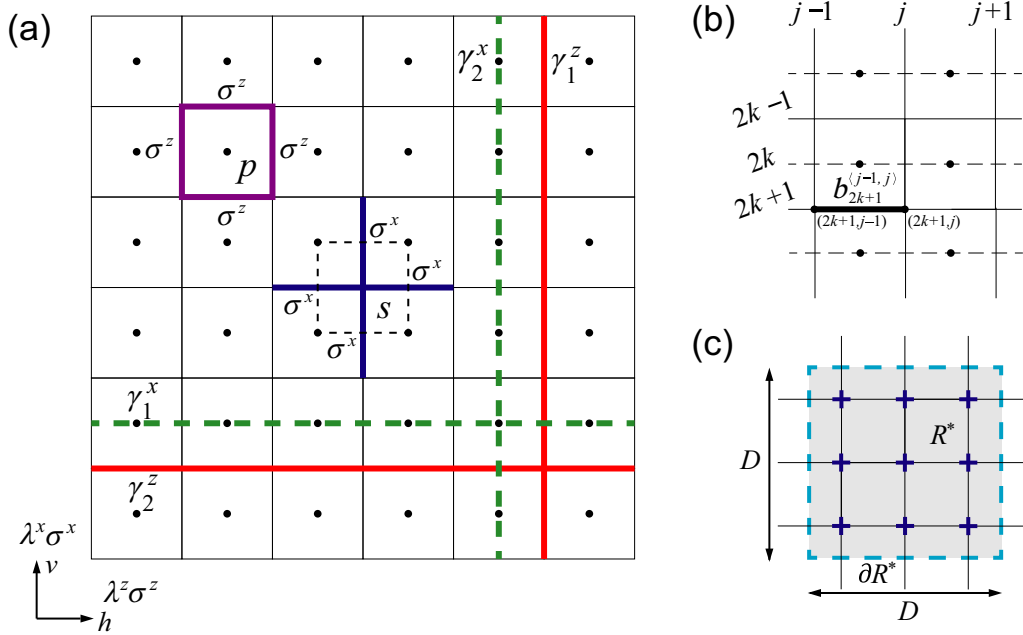


FIG. 1. (a) An $N \times N$ square lattice with periodic boundary conditions and spins- $\frac{1}{2}$ on the bonds. A star (s) on the lattice corresponds to a plaquette (p) on the dual lattice and vice versa. Fields in the z (x) direction with a magnitude of λ^z (λ^x) are located on the horizontal (vertical) edges. (b) An illustration of sites (i, j) , where the effective spins are located, and links $b_i^{(j-1, j)}$. (c) An illustration of the magnetic Wilson loop for a square region R^* , with $D = 3$. The region R^* contains $D \times D$ stars (dark blue crosses), and the boundary ∂R^* (light blue dashed line) threads $4D$ spins.

whose scaling behavior signals the topological QPTs. Furthermore, we show that thermalization and disorder-assisted stabilization of topological order after a quantum quench can be identified via multipartite entanglement. Using an upper bound of the QFI, we investigate the 2D TCM at finite temperatures and show that topological order cannot survive against thermal fluctuations in the thermodynamic limit.

Due to rapid developments of quantum techniques, recently two quantum simulation platforms [45,46] have generated topological order of the toric code type with several tens and several hundreds of qubits. Then, a practical witness of the long-range entanglement of the topologically ordered state is needed, which is relevant to the interests of experimentalists working on different quantum simulators. Here we propose an entanglement witness for the 2D TCM with the QFI in terms of averages of closed string operators, which are experimentally measurable [46]. Our work, based on the experimentally extractable QFI, will contribute to a deeper understanding of topological QPTs in condensed matter physics and has promising applications in both fault-tolerant quantum computation and robust quantum metrology [47].

II. TORIC CODE MODEL ON A TORUS WITH EXTERNAL FIELDS

The toric code model (TCM) has a resonating valence-bond phase [48] (aka a quantum spin liquid phase [1,3]) capturing all elements of topological order: \mathbb{Z}_2 excitations with anyonic particle statistics, a fourfold degenerate ground state on a torus, robustness against *local* perturbations, and no *local*-order parameter. Similar to the quantum dimer model on the Kagome lattice [49] and the Wen-plaquette model [50], the

2D TCM is a significant toy model for studying \mathbb{Z}_2 topological order. The Hamiltonian of the spin- $\frac{1}{2}$ TCM on a $N \times N$ square lattice reads [21,51]

$$\hat{H}_{\text{TC}} = -J^A \sum_s \hat{A}_s - J^B \sum_p \hat{B}_p, \quad (1)$$

where the stabilizer operators $\hat{A}_s \equiv \prod_{i \in \mathcal{S}_s} \hat{\sigma}_i^x$ and $\hat{B}_p \equiv \prod_{i \in \mathcal{P}_p} \hat{\sigma}_i^z$ both contain four spins belonging to a star s and a plaquette p , respectively [see Fig. 1(a)].

This model is exactly solvable, because all the star and plaquette operators commute with each other, i.e., $[\hat{A}_s, \hat{B}_p] = 0$ for $\forall s, p$. We have two constraints, $\prod_s \hat{A}_s = \prod_p \hat{B}_p = \mathbb{I}$, with periodic boundary conditions, and thus the ground state is fourfold degenerate, allowing for encoding two qubits. Any state in the ground-state manifold \mathcal{L} can be written as

$$|\mathcal{G}\rangle = \sum_{i,j=0}^1 a_{ij} |\xi_{ij}\rangle, \quad (2)$$

in terms of four bases

$$|\xi_{ij}\rangle = (\hat{W}_1^m)^i (\hat{W}_2^m)^j |\xi_{00}\rangle, \quad (3)$$

where we have $\sum_{i,j=0}^1 |a_{ij}|^2 = 1$, the string operators

$$\hat{W}_{1,2}^m \equiv \prod_{i \in \gamma_{1,2}^m} \hat{\sigma}_i^x, \quad (4)$$

and

$$|\xi_{00}\rangle \propto \prod_s (\mathbb{I} + \hat{A}_s) |\uparrow\rangle, \quad (5)$$

with $|\uparrow\rangle$ being the all spin-up state in the $\hat{\sigma}^z$ basis. The excitations of the TCM are in two categories: The electric charges (e) and the magnetic vortices (m) of a \mathbb{Z}_2 lattice gauge theory, which have nontrivial mutual statistics and follow fusion rules [21].

Then we consider the system (1) subsequently subject to the fields in the z and x directions on the horizontal and vertical edges, respectively [see Fig. 1(a)],

$$\hat{V} = - \sum_{i \in h} \lambda_i^z \hat{\sigma}_i^z - \sum_{j \in v} \lambda_j^x \hat{\sigma}_j^x. \quad (6)$$

The Hamiltonian of the TCM with external fields can be expressed as uncoupled Ising chains on different lines [52,53],

$$\hat{H}_{\text{tc}}^{\text{field}} = \hat{H}_{\text{tc}} + \hat{V} = \sum_{i=1}^{2N} \hat{H}_i, \quad (7)$$

where the transverse-field Ising Hamiltonian is

$$\hat{H}_i \equiv - \sum_{j=1}^N [J^{(i)} \hat{\tau}_{i,j}^x \hat{\tau}_{i,j+1}^x + \lambda_j^{(i)} \hat{\tau}_{i,j}^z], \quad (8)$$

with $\lambda_j^{(i)} = \lambda_j^z$ (λ_j^x) and $J^{(i)} = J^A$ (J^B) for i being odd (even), $[\hat{H}_i, \hat{H}_l] = 0$, and $\hat{\tau}_{i,j}^{x,z}$ being Pauli operators after applying the dual transformation (see Appendix A), on the site (i, j) of the original and dual lattice at the i th row and j th column [see Fig. 1(b) for the original lattice].

III. GAUGE-INVARIANT WILSON LOOP

A \mathbb{Z}_2 lattice gauge theory [54] has confined and deconfined phases and is equivalent to the classical Ising model. The TCM [44] can be mapped into the Hamiltonian of a \mathbb{Z}_2 lattice gauge theory [55], and the \mathbb{Z}_2 topological order (in the deconfined phase) can be probed via the expectation value of the gauge-invariant Wilson loop [54,56]. For a square region R^* on the dual lattice with $D \times D$ stars [see Fig. 1(c)], the Wilson loop is defined as the average of a magnetic closed string operator $\mathcal{W}_{R^*}^m \equiv \langle \hat{W}_{R^*}^m \rangle$ [44] with

$$\hat{W}_{R^*}^m = \prod_{i \in \partial R^*} \hat{\sigma}_i^x = \prod_{s \in R^*} \hat{A}_s, \quad (9)$$

where ∂R^* denotes the boundary of R^* . Similarly, the Wilson loop for a square region R on the original lattice, with $D \times D$ plaquettes, can be defined as $\mathcal{W}_R^e = \langle \hat{W}_R^e \rangle$ with an electric closed string operator

$$\hat{W}_R^e = \prod_{i \in \partial R} \hat{\sigma}_i^z = \prod_{p \in R} \hat{B}_p. \quad (10)$$

For simplicity, we consider the reduced Wilson loop, defined as

$$w_D^{e,m} \equiv (\mathcal{W}_D^{e,m})^{1/D}. \quad (11)$$

For a large square region with $D \gg 1$, the Wilson loops on both original and dual lattices follow a perimeter law

$$\mathcal{W}^{e,m} \propto \exp(-\beta D), \quad (12)$$

i.e., $w_D^{e,m} \rightarrow \text{const} \neq 0$, for the existence of topological order, and either or both follow an area law

$$\mathcal{W}^e \propto \exp(-\beta D^2) \text{ or/and } \mathcal{W}^m \propto \exp(-\beta D^2), \quad (13)$$

i.e., $w_D^e \rightarrow 0$ or/and $w_D^m \rightarrow 0$, when topological order is absent [44].

For the TCM with external fields, the reduced Wilson loop can be written as a spin-spin correlator for the ground state,

$$w_D^{e,m} = \langle \hat{\tau}_{i,j}^x \hat{\tau}_{i,j+D}^x \rangle_{\mathcal{G}}, \quad (14)$$

for i being even and odd, respectively. For simplicity, we consider uniform external fields $\lambda_j^{x,z} = \lambda^{x,z}$ and set $J_A = J_B = 1$. For the topologically trivial phase (λ^x or $\lambda^z > 1$), we have w_D^e or $w_D^m \rightarrow 0$; for the topologically nontrivial phase with topological order ($\lambda^{x,z} < 1$), we have $w_D^{e,m} \rightarrow \text{const} > 0$ [see Fig. 2(a)].

IV. PROBING TOPOLOGICAL ORDER IN THE TCM BY THE QFI DENSITY

Recent studies [39,40] show that multipartite entanglement, witnessed by the QFI with *nonlocal* operators, can characterize 1D SPT order and topological order in the Kitaev honeycomb model. For a pure state $|\psi\rangle$, the QFI, with respect to a generator \hat{O} , can be simply calculated as [31]

$$F_Q = 4(\Delta_\psi \hat{O})^2, \quad (15)$$

where $(\Delta_\psi \hat{O})^2 \equiv \langle \hat{O}^2 \rangle_\psi - \langle \hat{O} \rangle_\psi^2$. For an m -partite system, the QFI density, defined as

$$f_Q \equiv F_Q/m, \quad (16)$$

gives an entanglement criterion; the violation of the inequality $f_Q \leq \kappa$ signals $(\kappa + 1)$ -partite entanglement ($1 \leq \kappa \leq m - 1$) [57].

For the TCM with uniform external fields in the x, z directions, we consider the square regions with $L \times L$ spins on the original and dual lattices, respectively. The generators for the QFI are chosen as

$$\hat{O}^e = \sum_{k,j=1}^L \hat{\tau}_{2k,j}^x / 2, \quad \hat{O}^m = \sum_{k,j=1}^L \hat{\tau}_{2k-1,j}^x / 2 \quad (17)$$

for the regions on the original and dual lattices, respectively. We obtain two QFI densities:

$$f_Q[\hat{O}^{e,m}, |\mathcal{G}\rangle] \equiv F_Q[\hat{O}^{e,m}, |\mathcal{G}\rangle] / L^2 = 1 + \sum_{D=1}^{L-1} w_D^{e,m}, \quad (18)$$

which are expressed in terms of the reduced Wilson loops (14) for increasing sizes of the square regions on the original and dual lattices, respectively. As discussed in Refs. [34,39,40], the QFI densities, as a function of L , follow an asymptotic power-law scaling in the thermodynamic limit:

$$f_Q[\hat{O}^{e,m}, |\mathcal{G}\rangle] = 1 + \alpha^{e,m} L^{\beta^{e,m}}, \quad (19)$$

where the scaling coefficients $\alpha^{e,m}$ and $\beta^{e,m}$ depend on the parameters of the TCM with external fields. When $\beta^{e,m} \rightarrow 1$, multipartite entanglement, witnessed via the QFI densities, increase linearly with the side length L of the region, indicating the presence of long-range quantum correlations.

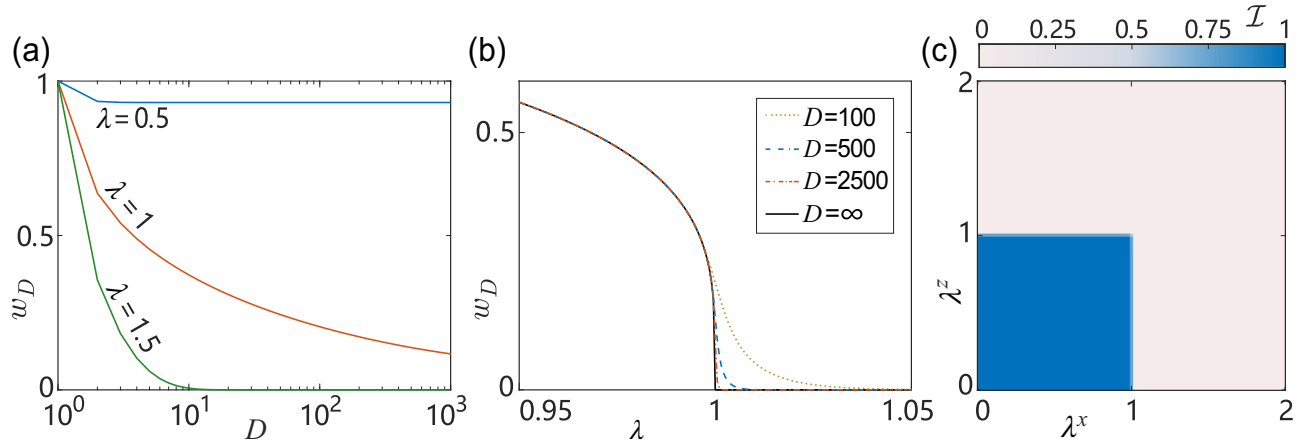


FIG. 2. (a) The reduced Wilson loop w_D as a function of the side length D of the square region on the lattice of the TCM for different strengths, $\lambda = 0.5, 1, 1.5$, of the external fields. (b) The reduced Wilson loop w_D in the vicinity of a quantum critical point $\lambda = 1$. (c) The scaling topological index $\mathcal{I} \equiv \beta^e \beta^m$ obtained from the QFI densities $f_Q[\mathcal{O}^{e,m}, |\mathcal{G}\rangle]$ of a chosen square region with a side length $L = 2000$ for different strengths $\lambda^{x,z}$ of external fields. The size of the square lattice of the TCM is $N \times N$ with $N = 5L = 10,000$.

Then, we can define a topological index as

$$\mathcal{I} \equiv \beta^e \times \beta^m, \quad (20)$$

combining the scaling behaviors of the QFI densities with respect to the generators (17) for the original and dual lattices, respectively. According to the scaling behavior of the Wilson loop, this topological index approximates 1 in the topological phase ($0 < \lambda^{x,z} < 1$) and vanishes in the topologically trivial phase ($\lambda^x > 1$ or $\lambda^z > 1$). Here the absence of *nonlocal* entanglement in the regions on the original lattice $\beta^e \simeq 0$ (dual lattice $\beta^m \simeq 0$) indicates the existence of many anyonic electric (magnetic) excitations characterized by the Wilson loop according to the \mathbb{Z}_2 lattice gauge theory. Thus $\mathcal{I} \rightarrow 1$, signaling multipartite entanglement with respect to the generators defined in both original and dual lattices, indicates the existence of topological order in the TCM with external fields, and $\mathcal{I} \rightarrow 0$ implies the absence of topological order. As shown in Fig. 2(c), the topological QPTs in the 2D TCM with external fields can be effectively characterized via multipartite entanglement.

V. OBSERVING THERMALIZATION OF THE TOPOLOGICAL STATE AFTER A QUANTUM QUENCH VIA MULTIPARTITE ENTANGLEMENT

Topological order, promising for topological quantum memories [58] and topological quantum computation [22], is believed to be robust against perturbations, which cannot change the topological nature of the ground state. However, topological order in the 2D TCM is not stable when kicked out of equilibrium [51,59] or at finite temperatures [60]. First, we use multipartite entanglement to study thermalization of the topological ground state of the TCM after a quantum quench with external fields. The system before the sudden quench ($t < 0$) is supposed to be in the topologically ordered ground state, $|\Psi_0\rangle = |\mathcal{G}_{\text{tc}}\rangle$, of the TCM with \hat{H}_{tc} in Eq. (1). At $t = 0$, the Hamiltonian is suddenly changed to $\hat{H}_{\text{tc}}^{\text{field}} = \hat{H}_{\text{tc}} + \hat{V}$, with \hat{V} in Eq. (6) being the uniform external fields in the x, z

directions ($\lambda_j^{x,z} = \lambda^{x,z}$). The system evolves as

$$|\Psi(t)\rangle = \exp(-it\hat{H}_{\text{tc}}^{\text{field}})|\mathcal{G}_{\text{tc}}\rangle, \quad (21)$$

and we focus on the stable state of the system at an infinite-long time ($t \rightarrow \infty$). In the thermodynamic limit $N \rightarrow \infty$, for a large chosen region of the original (dual) lattice $D \gg 1$, the long-time reduced Wilson loop can be calculated as (see Appendix B and Ref. [61])

$$w_D^{\text{e,m}} = \begin{cases} [(1 + \sqrt{1 - \lambda^2})/2]^D, & \text{for } 0 < \lambda^{x,z} \leq 1, \\ 1/2^D, & \text{for } \lambda^{x,z} > 1, \end{cases} \quad (22)$$

which decays to zero for $D \rightarrow \infty$, except for the case without quenched external fields $\lambda^x = \lambda^z = 0$. Thus for any nonzero quenched external field, λ^x or $\lambda^z \neq 0$, we can derive that the QFI density

$$f_Q[\hat{\mathcal{O}}^e, |\Psi(\infty)\rangle] = \text{const} \text{ or } f_Q[\hat{\mathcal{O}}^m, |\Psi(\infty)\rangle] = \text{const}, \quad (23)$$

leading to thermalization of topological order with a zero topological index $\mathcal{I} \simeq 0$ (see also Appendix B). Therefore thermalization of the topologically ordered state witnessed via multipartite entanglement implies that the quench of any transverse field is a source of fluctuations for destroying topological order in the TCM at zero temperature.

VI. DYNAMICAL LOCALIZATION OF THE TOPOLOGICALLY ORDERED STATE WITH DISORDER

We now investigate how to stabilize the topologically ordered state in the TCM using the multipartite entanglement witness. By introducing disorder in the coupling strengths of stabilizer operators [62–64], topological order can be protected from a quantum quench with external fields at zero temperature [65]. The Hamiltonian of the TCM with disordered coupling strengths reads

$$\hat{H}_{\text{tc}}^{\text{D/O}} = - \sum_s J_s^A \hat{A}_s - \sum_p J_p^B \hat{B}_p, \quad (24)$$

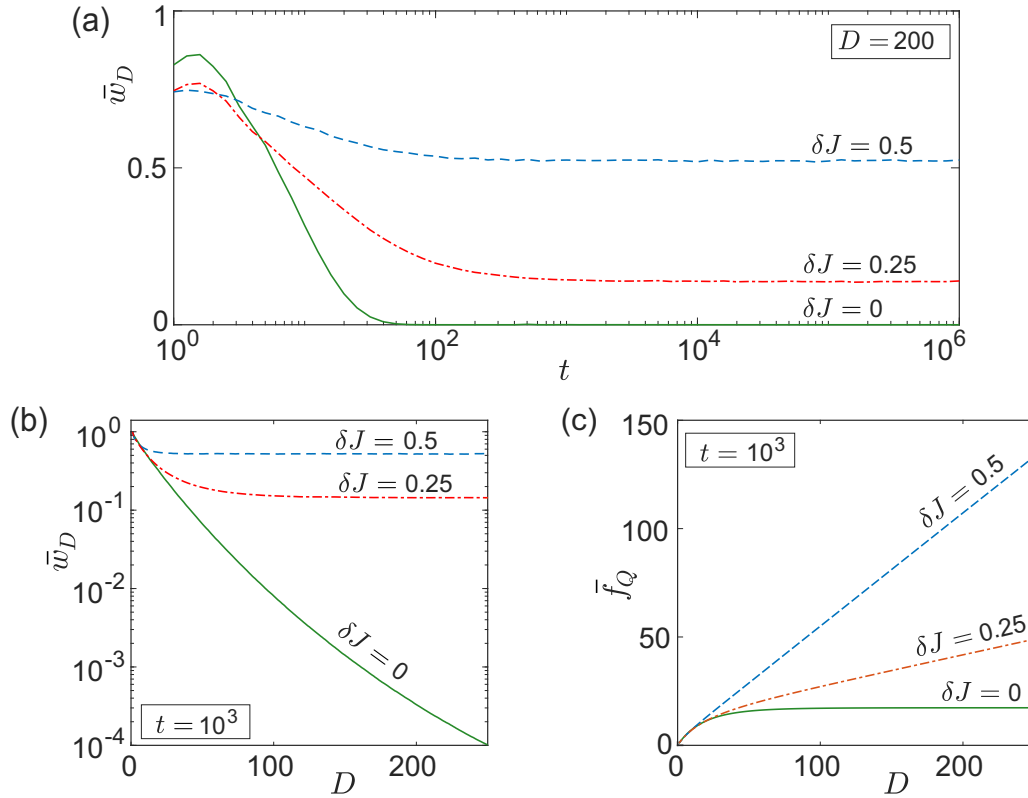


FIG. 3. Dynamical localization of topological order in the 2D TCM after a quantum quench. (a) Time evolutions of the average reduced Wilson loops \bar{w}_D for $\delta J = 0, 0.25, 0.5$ with a length D of the square region up to $L = 200$. (b) The average reduced Wilson loops \bar{w}_D versus the length D of the square region for $\delta J = 0, 0.25, 0.5$ at $t = 10^3$. (c) The average QFI densities \bar{f}_Q versus the length D of the square region for $\delta J = 0, 0.125, 0.25, 0.5$ at $t = 10^3$. The side length of the square lattice is $N = 5L = 1000$, and the number of realizations of disordered coupling strengths is 1000.

where the random coupling strengths $J_s^A = J^A + \delta J_s^A$ and $J_p^B = J^B + \delta J_p^B$ are applied, with $\delta J_s^A \in [-\delta J^A, \delta J^A]$ and $\delta J_p^B \in [-\delta J^B, \delta J^B]$. Given $J^{A,B} > 0$ and $0 < \delta J^{A,B} < 1$, the system is stable in the same ground-state $|\mathcal{G}_{\text{tc}}\rangle$ of the TCM (1) at zero temperature. At time $t = 0$, the sudden quench dynamics occurs by adding external fields \hat{V} (6) at $t = 0$. It has been demonstrated in Ref. [65] that in the presence of disorder in the coupling strengths of stabilizer operators, the quantum quench is equivalent to a quasiadiabatic evolution with a family of *local* Hamiltonians, and the quenched state

$$|\Psi(t)\rangle = \exp[-i(\hat{H}_{\text{tc}}^{\text{D/O}} + \hat{V})t]|\mathcal{G}_{\text{tc}}\rangle \quad (25)$$

and the initial ground-state $|\mathcal{G}_{\text{tc}}\rangle$ belong to the same topological phase [66–69]. Therefore after a quantum quench, dynamical localization, induced by disorder, can preserve the ground-state degeneracy, energy gap, and topological order robustness [65].

We now numerically investigate the dynamical localization of topological order by considering multipartite entanglement of the time-evolved state (see Appendix C). Without loss of generality, we set $J^{A,B} = 1$, consider the same disorder strength $\delta J^{A,B} = \delta J$, and choose the strengths of the quenched fields in Eq. (6) as $\lambda_i^z = \lambda_j^x = 0.5$. In Fig. 3(a), we plot the time evolutions of the average reduced Wilson loops \bar{w}_D over 1000 realizations of disorder coupling strengths with a length of the square region up to $L = 200$ and a length of the square

lattice being $N = 5L = 1000$. For long-time evolutions, the average reduced Wilson loops converge to a finite value (with disorder), or exponentially decay (without disorder). For long times (e.g., $t = 10^3$), the average Wilson loops of the stable states follow a perimeter law (with disorder) or an area law (without disorder) [see Fig. 3(b)]. Thus the average QFI densities $\bar{f}_Q \propto L$ (with disorder) or $\bar{f}_Q \rightarrow \text{const}$ (without disorder) [see Fig. 3(c)].

In addition to the numerical results using topological entanglement entropy [65], we show that the stable states have the same scaling behaviors of multipartite entanglement as the topological ground states of the TCM. These results manifest that these two kinds of states belong to the same topological phase, and topological order can be protected from a quantum quench by introducing disorder.

VII. ABSENCE OF TOPOLOGICAL ORDER IN THE THERMODYNAMIC LIMIT AT ANY FINITE TEMPERATURE

Since the topological entanglement entropy cannot distinguish quantum correlations from classical ones for a mixed thermal state, it has attracted growing interest to search for an order parameter, based on a mixed-state entanglement detection, for finite-temperature topological order [70–72]. Here using the QFI as an effective entanglement witness for a mixed state [33,73], we investigate whether topological order can

survive in the 2D TCM against thermal fluctuations at finite temperatures.

For a mixed state ρ with all possible pure-state ensembles $\{p_l, |\phi_l\rangle\}$, the QFI is given by the convex roof of the averaged variance of the generator \hat{O} [74], i.e.,

$$F_Q[\hat{O}, \rho] = 4 \min_{\{p_l, |\phi_l\rangle\}} \sum_l p_l (\Delta_{\phi_l} \hat{O})^2. \quad (26)$$

To better approximate the QFI of a thermal state of the TCM at finite temperatures, we use the minimally entangled typical quantum states (METTS) [75] to decompose the thermal state as [34,76]

$$\rho_T = \exp(-\hat{H}_{\text{tc}}/T) / \mathcal{Z} = \sum_i p_l |\phi_l\rangle \langle \phi_l|, \quad (27)$$

where $\mathcal{Z} \equiv \text{Tr}[\exp(-\hat{H}_{\text{tc}}/T)]$ and $p_l = \langle l | \rho_T | l \rangle$. Here

$$|\phi_l\rangle = \exp[-\hat{H}_{\text{tc}}/(2T)] |l\rangle / \sqrt{p_l} \quad (28)$$

is the METTS by taking $|l\rangle$ as a product state. The central idea of METTS is to break a thermal state with inverse temperature $1/T$ into two copies of the thermal state with $1/(2T)$ [75].

For the square region R^* on the dual lattice, we choose $|l\rangle$ as a product state in the $\hat{\sigma}^z$ basis and have

$$|\phi_l\rangle \propto \exp \left[J^A \sum_s \hat{A}_s / (2T) \right] |l\rangle. \quad (29)$$

The QFI density is upper bounded as (see Appendix D)

$$f_Q[\hat{O}^m, \rho_T] \leq 1 + \sum_{D=1}^{L-1} \tanh(J^A/T)^D, \quad (30)$$

which converges to a constant for any nonzero temperature $T > 0$ in the thermodynamic limit $L \rightarrow \infty$. Similarly, for the region R on the original lattice, we choose $|l'\rangle$ to be the product state in the $\hat{\sigma}^x$ axis, and the QFI density is upper bounded as

$$f_Q[\hat{O}^e, \rho_T] \leq 1 + \sum_{D=1}^{L-1} \tanh(J^B/T)^D, \quad (31)$$

which converges to a constant for $T > 0$ and $L \rightarrow \infty$. Moreover, with these upper bounds, we can simply deduce that the scaling coefficients of the QFI densities, defined in Eq. (19), are both equal to zero, $\beta^{\text{e,m}} = 0$, with a zero topological index, $\mathcal{I} = 0$, at any finite temperature. Therefore we conclude that multipartite entanglement, witnessed via the QFI, can detect the absence of finite-temperature topological order in the 2D TCM in the thermodynamic limit, which agrees with the result obtained using negativity [72].

VIII. CONCLUSIONS

We demonstrated that the QFI, as a witness of multipartite entanglement, can characterize topological QPTs in the TCM on a square lattice with external fields. The QFI density of the ground state is expressed in terms of the expectation values of reduced Wilson loops for different sizes of square regions, of which the scaling behavior identifies the \mathbb{Z}_2 topological order. Moreover, the QFI can be used to study

thermalization and disorder-assisted stabilization of topological order after a quantum quench. Last, the convex roof of the QFI is applied to investigate the TCM at finite temperatures, showing that topological order cannot survive at any nonzero temperature in the thermodynamic limit. Using the experimentally extractable QFI, our results will help to study topological QPTs in condensed matter physics with promising applications in fault-tolerant quantum computation and robust quantum metrology. In addition, it was recently shown in Ref. [77] that regardless of a specific type of quantum resource, the QFI identifies every resourceful quantum state in general quantum resource theories [78]. Our results would also inspire further investigations of the quantum resources of topological quantum states for additional applications with quantum advantages.

ACKNOWLEDGMENTS

We thank Dr. Zi-Yong Ge for useful discussions. Y.R.Z. is partially supported by the Japan Society for the Promotion of Science (JSPS) (via Postdoctoral Fellowship Grant No. P19326, and the Grants-in-Aid for Scientific Research (KAKENHI) Grant No. JP19F19326). H.F. is partially supported by the National Natural Science Foundation of China (NSFC) (Grants No. T2121001 and 11934018), and the Strategic Priority Research Program of Chinese Academy of Sciences (Grant No. XDB28000000). T.L. thanks the support from the startup grant of South China University of Technology. J.Q.Y. is partially supported by the National Key Research and Development Program of China (Grant No. 2016YFA0301200), the National Natural Science Foundation of China (NSFC) (Grants No. 11934010 and No. U1801661), and the Zhejiang Province Program for Science and Technology (Grant No. 2020C01019). F.N. is supported in part by Nippon Telegraph and Telephone Corporation (NTT) Research, the Japan Science and Technology Agency (JST) [via the Quantum Leap Flagship Program (Q-LEAP), and the Moonshot R&D Grant No. JPMJMS2061], the Japan Society for the Promotion of Science (JSPS) [via the Grants-in-Aid for Scientific Research (KAKENHI) Grant No. JP20H00134], the Army Research Office (ARO) (Grant No. W911NF-18-1-0358), the Asian Office of Aerospace Research and Development (AOARD) (via Grant No. FA2386-20-1-4069), and the Foundational Questions Institute Fund (FQXi) (via Grant No. FQXi-IAF19-06).

APPENDIX A: TRANSFORMING THE TCM TO UNCOUPLED TRANSVERSE ISING CHAINS VIA DUAL TRANSFORMATIONS

The Hamiltonian of the TCM with external fields can be divided into two mutually commutative parts,

$$\hat{H}_{\text{tc}}^{\text{field}} \equiv \hat{H}_{\text{tc}} + \hat{V} = \hat{H}^A + \hat{H}^B, \quad (A1)$$

with $[\hat{H}^A, \hat{H}^B] = 0$, where

$$\hat{H}^A = -J^A \sum_s \hat{A}_s - \lambda_z \sum_{i \in h} \hat{\sigma}_i^z, \quad (A2)$$

$$\hat{H}^B = -J^B \sum_p \hat{B}_p - \lambda_x \sum_{i \in v} \hat{\sigma}_i^x. \quad (A3)$$

For clarity, (i, j) denotes the site of the original lattice and the dual lattice at row i and column j ; $b_i^{(j, j+1)}$ denotes the bond connecting two sites (i, j) and $(i, j+1)$. For an odd row $i = 2k-1$, $(2k-1, j)$ belongs to the original lattice, while for an even row $i = 2k$, $(2k-1, j)$ is located on the dual lattice [see Fig. 1(b)]. By introducing the effective spins with Pauli operators via the dual transformations,

$$\hat{\tau}_{2k-1, j}^x = \prod_{l \leq j} \hat{A}_{2k-1, l}, \quad \hat{\tau}_{2k-1, j}^z = \hat{\sigma}_{b_{2k-1}^{(j, j+1)}}^z, \quad (\text{A4})$$

on the lattice site $(2k-1, j)$, \hat{H}^A becomes [51]

$$\hat{H}^A = \sum_{k=1}^N \hat{H}_{2k-1}, \quad (\text{A5})$$

with

$$\hat{H}_{2k-1} = - \sum_{j=1}^N (J^A \hat{\tau}_{2k-1, j}^x \hat{\tau}_{2k-1, j+1}^x + \lambda_j^z \hat{\tau}_{2k-1, j}^z). \quad (\text{A6})$$

Similarly, we can introduce effective spins on the dual lattice with Pauli operators via the dual transformations:

$$\hat{\tau}_{2k, j}^x = \prod_{l \leq j} \hat{B}_{2k, l}, \quad \hat{\tau}_{2k, j}^z = \hat{\sigma}_{b_{2k}^{(j, j+1)}}^x, \quad (\text{A7})$$

with which \hat{H}^B is expressed as

$$\hat{H}^B = \sum_{k=1}^N \hat{H}_{2k}, \quad (\text{A8})$$

where

$$\hat{H}_{2k} = - \sum_{j=1}^N (J^B \hat{\tau}_{2k, j}^x \hat{\tau}_{2k, j+1}^x + \lambda_j^z \hat{\tau}_{2k, j}^z). \quad (\text{A9})$$

APPENDIX B: WILSON LOOP IN THE TCM AFTER A QUANTUM QUENCH

In the previous section, we show that using the dual transformations, the Hamiltonian of the TCM with external fields can be expressed as uncoupled transverse-field Ising chains on different lines. Therefore the out-of-equilibrium dynamics of the TCM can be investigated using the results of the transverse-field Ising chain.

We consider a quantum quench of a transverse-field Ising chain at its ground state with a Hamiltonian:

$$\hat{H}_{\text{Ising}} = - \sum_{j=1}^N [\hat{\tau}_j^x \hat{\tau}_{j+1}^x + \lambda(t) \hat{\tau}_j^z], \quad (\text{B1})$$

where the transverse field is changed from λ_0 to λ abruptly at time $t = 0$

$$\lambda(t) = \begin{cases} \lambda_0, & \text{for } t \leq 0 \\ \lambda, & \text{for } t > 0 \end{cases}. \quad (\text{B2})$$

It can be rewritten in terms of the Jordan-Wigner transformation

$$\hat{\tau}_j^z = (2\hat{c}_j^\dagger \hat{c}_j - 1), \quad \hat{\tau}_j^+ = \hat{c}_j^\dagger \prod_{l=1}^{j-1} (1 - 2\hat{c}_l^\dagger \hat{c}_l), \quad \hat{\tau}_1^+ = \hat{c}_1^\dagger,$$

as

$$\hat{H}_{\text{Ising}} = \sum_j [(\hat{c}_j - \hat{c}_j^\dagger)(\hat{c}_{j+1}^\dagger + \hat{c}_{j+1}) - \lambda(\hat{c}_j^\dagger \hat{c}_j - \hat{c}_j \hat{c}_j^\dagger)]. \quad (\text{B3})$$

In the thermodynamic limit $N \gg 1$, we use the Fourier transformation (with q being the wave vector),

$$\hat{c}_j = \sum_q e^{-iqj} \hat{c}_q / \sqrt{N}, \quad (\text{B4})$$

to obtain the Bogoliubov-de Gennes Hamiltonian of a transverse-field Ising chain,

$$\hat{H}_{\text{Ising}} = \sum_q \mathbb{C}_q^\dagger \mathcal{H}_q \mathbb{C}_q, \quad (\text{B5})$$

with $\mathbb{C}_q^\dagger \equiv (\hat{c}_q^\dagger, \hat{c}_{-q})$, $y_q \equiv -\sin q$, $z_q \equiv -\lambda - \cos q$, $\tan \Theta_q \equiv y_q / z_q$, and

$$\mathcal{H}_q = \begin{pmatrix} -\lambda - \cos q & i \sin q \\ -i \sin q & \lambda + \cos q \end{pmatrix} = y_q \hat{\sigma}^y + z_q \hat{\sigma}^z. \quad (\text{B6})$$

The Hamiltonian can be diagonalized by using the Bogoliubov transformation as

$$\hat{H}_{\text{Ising}} = \sum_q \omega_q \mathbb{E}_q^\dagger \hat{\sigma}^z \mathbb{E}_q, \quad (\text{B7})$$

with $\mathbb{C}_q = \mathbb{R}_q \mathbb{E}_q$, $\omega_q = (y_q^2 + z_q^2)^{\frac{1}{2}}$, $\mathbb{E}_q^\dagger \equiv (\hat{\eta}_q^\dagger, \hat{\eta}_{-q})$,

$$\mathbb{R}_q = \begin{pmatrix} u_q & -iv_q \\ -iv_q & u_q \end{pmatrix}, \quad (\text{B8})$$

$u_q \equiv \cos \frac{\Theta_q}{2}$, and $v_q \equiv \sin \frac{\Theta_q}{2}$.

The Heisenberg equation of $\mathbb{C}_q(t)$ can be expressed as

$$i\partial_t \mathbb{C}_q(t) = 2\mathcal{H}_q \mathbb{C}_q(t). \quad (\text{B9})$$

We then define the time-propagation transformation of $\mathbb{C}_q(t)$ in terms of $\mathbb{E}_q(0)$ as $\mathbb{C}_q(t) = \mathbb{S}_q(t) \mathbb{E}_q(0)$, where

$$\mathbb{S}_q(t) = \begin{pmatrix} U_q(t) & -V_q^*(t) \\ V_q(t) & U_q^*(t) \end{pmatrix}. \quad (\text{B10})$$

Substituting it into the Heisenberg equation (B9), we can obtain

$$i\partial_t \mathbb{S}_q(t) = 2\mathcal{H}_q(g) \mathbb{S}_q(t). \quad (\text{B11})$$

With the initial constraints $U_q(0) = u_q(0) \equiv u_0$ and $V_q(0) = -iv_q(0) \equiv -iv_0$, the solutions of Eq. (B11) can be obtained as

$$\begin{pmatrix} U_q(t) \\ V_q(t) \end{pmatrix} = \begin{pmatrix} u_0 \cos 2\omega t + \frac{i \sin 2\omega t (zu_0 + yv_0)}{\omega} \\ -iv_0 \cos 2\omega t + \frac{\sin 2\omega t (yu_0 + zv_0)}{\omega} \end{pmatrix}, \quad (\text{B12})$$

where $\omega \equiv \omega_q(g)$, $y \equiv y_q(g)$, and $z \equiv z_q(g)$.

To calculate the reduced Wilson loop, written as an x -directional spin-correlation function [Eq. (5)], we need to consider two kinds of operators, $\hat{A}_j(t) = \hat{a}_j^\dagger(t) + \hat{a}_j(t)$ and $\hat{B}_j(t) = \hat{b}_j^\dagger(t) - \hat{b}_j(t)$, where

$$\hat{a}_j(t) = \sum_q e^{iqj} [U_q(t) + V_q(t)] \hat{\eta}_q(0) / \sqrt{N}, \quad (\text{B13})$$

$$\hat{b}_j(t) = \sum_q e^{iqj} [U_q(t) - V_q(t)] \hat{\eta}_q(0) / \sqrt{N}. \quad (\text{B14})$$

According to Wick's theorem, we only need to consider three types of contraction [51],

$$\begin{aligned} G_r(t) &\equiv \langle \mathcal{G}(0) | \hat{\mathcal{B}}_j(t) \hat{\mathcal{A}}_{j+r}(t) | \mathcal{G}(0) \rangle \\ &= \sum_q \frac{e^{-iqr}}{N} \left[\frac{z_0 z + y_0 y}{(iy - z)\omega_0} + i \frac{z_0 y - z y_0}{(iy - z)\omega_0} \cos 4\omega t \right], \end{aligned} \quad (\text{B15})$$

$$\begin{aligned} G_r^A(t) &\equiv \langle \mathcal{G}(0) | \hat{\mathcal{A}}_j(t) \hat{\mathcal{A}}_{j+r}(t) | \mathcal{G}(0) \rangle \\ &= \delta_{r,0} + \sum_q \frac{e^{-iqr}}{N} \frac{z_0 y - z y_0}{\omega \omega_0} \sin 4\omega t, \end{aligned} \quad (\text{B16})$$

$$\begin{aligned} G_r^B(t) &\equiv \langle \mathcal{G}(0) | \hat{\mathcal{B}}_j(t) \hat{\mathcal{B}}_{j+r}(t) | \mathcal{G}(0) \rangle \\ &= -\delta_{r,0} + \sum_q \frac{e^{-iqr}}{N} \frac{z_0 y - z y_0}{\omega \omega_0} \sin 4\omega t. \end{aligned} \quad (\text{B17})$$

The x -directional spin-correlation function, expressed as a Pfaffian, can be calculated. Details of the calculation can be found in Refs. [61,79].

We consider the quench from the ground state of the toric code $\lambda_0 = 0$ to the case with $\lambda_f = \lambda$. In the long-time limit ($t \rightarrow \infty$) and thermodynamic limit ($\frac{1}{N} \sum_q \rightarrow \frac{1}{2\pi} \int dq$), the time-dependent oscillating terms vanish, and therefore we can obtain that $G_r^A = \delta_{r,0}$, $G_r^B = -\delta_{r,0}$, for $\lambda < 1$

$$G_r(\infty) = \begin{cases} (1 - \lambda^2)\lambda^{r-1}/2, & \text{for } r \geq 2 \\ 1 - \lambda^2/2, & \text{for } r = 1 \\ -\lambda/2, & \text{for } r = 0 \\ 0, & \text{for } r \leq -1 \end{cases}, \quad (\text{B18})$$

and for $\lambda > 1$

$$G_r(\infty) = \begin{cases} 0, & \text{for } r \geq 2 \\ 1/2, & \text{for } r = 1 \\ -1/(2\lambda), & \text{for } r = 0 \\ (\lambda^2 - 1)\lambda^{r-1}/2, & \text{for } r \leq -1 \end{cases}, \quad (\text{B19})$$

by using the residue theorem. Furthermore, the x -directional spin-correlation function $C_d^x(\infty) \equiv \langle \sigma_j^x(\infty) \sigma_{j+d}^x(\infty) \rangle_{\mathcal{G}}$ (without loss of generality, we assume that $d \geq 0$) reduces to a determinant

$$C_d^x(\infty) = \begin{vmatrix} G_1(\infty) & G_0(\infty) & \cdots & G_{-d+2}(\infty) \\ G_2(\infty) & G_1(\infty) & \cdots & G_{-d+3}(\infty) \\ \vdots & \vdots & \ddots & \vdots \\ G_d(\infty) & G_{d-1}(\infty) & \cdots & G_1(\infty) \end{vmatrix}. \quad (\text{B20})$$

For $\lambda > 1$, we can obtain that $C_d^x(\infty) = 1/2^d$, which decays exponentially with respect to the distance d . For $0 < \lambda < 1$, the result becomes [80]

$$C_d^x(\infty) = \frac{\lambda^{d+1}}{2^d} \cosh \left[(d+1) \log \frac{1 + \sqrt{1 - \lambda^2}}{\lambda} \right], \quad (\text{B21})$$

which for $d \rightarrow \infty$ becomes

$$C_d^x(\infty) \rightarrow \left(\frac{1 + \sqrt{1 - \lambda^2}}{2} \right)^{d+1}. \quad (\text{B22})$$

APPENDIX C: NUMERICAL EVIDENCE FOR DYNAMICAL LOCALIZATION OF TOPOLOGICAL ORDER IN A DISORDERED TCM

Here we consider a disordered Ising chain with the Hamiltonian:

$$\hat{H}^{D/O} = - \sum_j (J_j \hat{\tau}_j^x \hat{\tau}_{j+1}^x + \lambda_j \hat{\tau}_j^z). \quad (\text{C1})$$

It can be rewritten in terms of the Jordan-Wigner transformation

$$\hat{\tau}_j^z = (2\hat{c}_j^\dagger \hat{c}_j - 1), \quad \hat{\tau}_j^+ = \hat{c}_j^\dagger \prod_{l=1}^{j-1} (1 - 2\hat{c}_l^\dagger \hat{c}_l), \quad \hat{\tau}_1^+ = \hat{c}_1^\dagger,$$

as

$$\begin{aligned} \hat{H}^{D/O} &= \sum_j [J_j (\hat{c}_j - \hat{c}_j^\dagger) (\hat{c}_{j+1}^\dagger + \hat{c}_{j+1}) - \lambda_j (\hat{c}_j^\dagger \hat{c}_j - \hat{c}_j \hat{c}_j^\dagger)] \\ &= \frac{1}{2} \mathbb{C}^\dagger \mathbb{M} \mathbb{C}, \end{aligned} \quad (\text{C2})$$

where

$$\mathbb{C}^\dagger = (\hat{c}_1^\dagger, \dots, \hat{c}_N^\dagger, \hat{c}_1, \dots, \hat{c}_N),$$

and

$$\mathbb{M} = \begin{pmatrix} \mathbb{A} & \mathbb{B} \\ \mathbb{B}^T & -\mathbb{A} \end{pmatrix},$$

with \mathbb{A} and \mathbb{B} being $N \times N$ matrices of elements: $\mathbb{A}_{j,j} = 2\lambda_j$, $\mathbb{A}_{j,j+1} = \mathbb{A}_{j+1,j} = -J_j$, $\mathbb{B}_{j,j+1} = -\mathbb{B}_{j+1,j} = -J_j$, and boundary conditions $\mathbb{A}_{N,1} = \mathbb{A}_{1,N} = J_N$, $\mathbb{B}_{N,1} = -\mathbb{B}_{1,N} = J_N$ for even parity. By diagonalizing the matrix $\mathbb{R} \mathbb{M} \mathbb{R}^T = \mathbb{V}$, the Hamiltonian can be diagonalized as

$$\hat{H}^{D/O} = \frac{1}{2} \mathbb{E}^\dagger \mathbb{V} \mathbb{E} = \sum_j \omega_j (\hat{\eta}_j^\dagger \hat{\eta}_j - 1/2), \quad (\text{C3})$$

where $\mathbb{C} = \mathbb{R}^T \mathbb{E}$ with the orthogonal matrix

$$\mathbb{R} = \begin{pmatrix} \mathbb{G} & \mathbb{H} \\ \mathbb{H} & \mathbb{G} \end{pmatrix},$$

$$\mathbb{E}^\dagger = (\hat{\eta}_1^\dagger, \dots, \hat{\eta}_L^\dagger, \hat{\eta}_1, \dots, \hat{\eta}_L),$$

and

$$\mathbb{V} = \begin{pmatrix} \mathbb{W} & \\ & -\mathbb{W} \end{pmatrix},$$

with the diagonal matrix $\mathbb{W} = \text{diag}(\omega_1, \dots, \omega_N)$.

Similarly, the Heisenberg equation of $\hat{\eta}_j(t)$ is expressed as

$$i\partial_t \hat{\eta}_j(t) = i[\hat{H}^{D/O}, \hat{\eta}_j(t)] = -i\omega_j \hat{\eta}_j, \quad (\text{C4})$$

of which the solution can be expressed as

$$\mathbb{E}(t) = \begin{pmatrix} e^{-i\mathbb{W}t} & \\ & e^{i\mathbb{W}t} \end{pmatrix} \mathbb{E} = \exp(-i\mathbb{V}t) \mathbb{E}. \quad (\text{C5})$$

Considering that an initial Hamiltonian $\hat{H}_0^{D/O}$ is quenched to the new Hamiltonian $\hat{H}^{D/O}$, we have

$$\mathbb{C}(t) = \mathbb{R}^T \exp(-i\mathbb{V}t) \mathbb{R} \mathbb{C}_0, \quad (\text{C6})$$

where \mathbb{R} and \mathbb{V} are for the quenched Hamiltonian $\hat{H}^{D/O}$, \mathbb{C}_0 is for the initial Hamiltonian $\hat{H}_0^{D/O}$, and $\langle \cdots \rangle_{\mathcal{G}}$ denotes the average with the ground state of the initial Hamiltonian $\hat{H}_0^{D/O}$.

Then, the x -directional spin-correlation function $C_d^x(t) \equiv \langle \sigma_j^x(t) \sigma_{j+d}^x(t) \rangle_{\mathcal{G}}$ (without loss of generality, we assume that $d \geq 0$) can be expressed as

$$C_d^x(t) = \langle \hat{\mathcal{B}}_j(t) \hat{\mathcal{A}}_{j+1}(t) \hat{\mathcal{B}}_{j+1}(t) \cdots \hat{\mathcal{B}}_{j+d-1}(t) \hat{\mathcal{A}}_{j+d}(t) \rangle_{\mathcal{G}}, \quad (\text{C7})$$

where $\hat{\mathcal{A}}_j \equiv \hat{c}_j^\dagger + \hat{c}_j$ and $\hat{\mathcal{B}}_j \equiv \hat{c}_j^\dagger - \hat{c}_j$. Using Wick's theorem, the spin-correlation function can be written as a Pfaffian of a skew-symmetric matrix \mathbb{T}

$$C_d^x(t) = \text{pf}[\mathbb{T}(j, j+d, t)]. \quad (\text{C8})$$

The skew-symmetric matrix $\mathbb{T}(i, j, t)$ is defined as

$$\mathbb{T}(i, j, t) \equiv \begin{pmatrix} \mathbb{P}(i, j, t) & \mathbb{M}(i, j, t) \\ -\mathbb{M}(i, j, t)^T & \mathbb{Q}(i, j, t) \end{pmatrix}, \quad (\text{C9})$$

of which the elements of the submatrices are

$$\mathbb{P}_{mn}(i, j, t) = \delta_{mn} + \langle \hat{\mathcal{B}}_{j+m-1}(t) \hat{\mathcal{B}}_{j+n-1}(t) \rangle_{\mathcal{G}}, \quad (\text{C10})$$

$$\mathbb{Q}_{mn}(i, j, t) = -\delta_{mn} + \langle \hat{\mathcal{A}}_{j+m}(t) \hat{\mathcal{A}}_{j+n}(t) \rangle_{\mathcal{G}}, \quad (\text{C11})$$

$$\mathbb{M}_{mn}(i, j, t) = \langle \hat{\mathcal{B}}_{j+m-1}(t) \hat{\mathcal{A}}_{j+n}(t) \rangle_{\mathcal{G}}. \quad (\text{C12})$$

By expanding $\hat{\mathcal{A}}_j(t)$ and $\hat{\mathcal{B}}_j(t)$ with Eq. (C6), we have

$$\langle \hat{\mathcal{A}}_m(t) \hat{\mathcal{A}}_n(t) \rangle_{\mathcal{G}} = [\tilde{\Phi}(t) \tilde{\Phi}(t)^\dagger]_{mn}, \quad (\text{C13})$$

$$\langle \hat{\mathcal{B}}_m(t) \hat{\mathcal{B}}_n(t) \rangle_{\mathcal{G}} = -[\tilde{\Psi}(t) \tilde{\Psi}(t)^\dagger]_{mn}, \quad (\text{C14})$$

$$\langle \hat{\mathcal{A}}_m(t) \hat{\mathcal{B}}_n(t) \rangle_{\mathcal{G}} = [\tilde{\Phi}(t) \tilde{\Psi}(t)^\dagger]_{mn}, \quad (\text{C15})$$

$$\langle \hat{\mathcal{B}}_m(t) \hat{\mathcal{A}}_n(t) \rangle_{\mathcal{G}} = -[\tilde{\Psi}(t) \tilde{\Phi}(t)^\dagger]_{mn}, \quad (\text{C16})$$

with

$$\tilde{\Phi}(t) = \Phi^T \cos(\mathbb{W}t) \Phi \Phi_0^T - i \Phi^T \sin(\mathbb{W}t) \Psi \Psi_0^T, \quad (\text{C17})$$

$$\tilde{\Psi}(t) = \Psi^T \cos(\mathbb{W}t) \Psi \Psi_0^T - i \Psi^T \sin(\mathbb{W}t) \Phi \Phi_0^T, \quad (\text{C18})$$

where

$$\Phi = \mathbb{G} + \mathbb{H}, \quad \Psi = \mathbb{G} - \mathbb{H}$$

are for the quenched Hamiltonian $\hat{H}^{D/O}$, and

$$\Phi_0 = \mathbb{G}_0 + \mathbb{H}_0, \quad \Psi_0 = \mathbb{G}_0 - \mathbb{H}_0$$

are for the initial Hamiltonian $\hat{H}_0^{D/O}$. Therefore the evolution of the reduced Wilson loop [Eq. (5) in the main text] can be numerically simulated by calculating the Pfaffian (C8) of a matrix (C9) with elements (C10)–(C12) using (C13)–(C16) with equations of evolutions (C17), (C18) (see also Ref. [65]).

APPENDIX D: UPPER BOUND OF THE QFI OF THE THERMAL STATE OF THE TCM

The thermal state of the TCM at temperature T with a Hamiltonian in Eq. (1) in the main text can be factorized

as

$$\rho_T = \frac{e^{-\hat{H}_{\text{tc}}/T}}{\mathcal{Z}} \quad (\text{D1})$$

$$\sim \prod_s [1 + \tanh(J^A/T) \hat{A}_s] \prod_p [1 + \tanh(J^B/T) \hat{B}_p], \quad (\text{D2})$$

with the partition function being $\mathcal{Z} = \text{Tr}[\exp(-\hat{H}_{\text{tc}}/T)]$.

To obtain the upper bound of the QFI [Eq. (11) in the main text] with respect to the generator $\hat{\mathcal{O}}^m$ [Eq. (6) in the main text], we first choose the state $|l\rangle$ as a product state in the $\hat{\sigma}^z$ basis, and the METTS is expressed as

$$|\phi_l\rangle = \rho_T^{1/2} |l\rangle / \sqrt{p_l} \sim \prod_s [1 + \tanh(J^A/(2T)) \hat{A}_s] |l\rangle, \quad (\text{D3})$$

with $p_l = \langle l | \rho_T | l \rangle$. Then, we calculate the average variance of the generator $\hat{\mathcal{O}}^m$ [Eq. (6) in the main text] for the METTSs $\{|\phi_l\rangle\}$ as

$$F_Q[\hat{\mathcal{O}}^m, \rho_T] \leq \sum_l p_l (\Delta_{\phi_l} \hat{\mathcal{O}}^m)^2 \quad (\text{D4})$$

$$\begin{aligned} &= L^2 \sum_l p_l \left(1 + \sum_{D=1}^{L-1} \langle \phi_l | \hat{\tau}_1^x \hat{\tau}_{1+D}^x | \phi_l \rangle \right) \\ &= L^2 \left(1 + \sum_{D=1}^{L-1} \sum_l p_l \langle \phi_l | \hat{\tau}_1^x \hat{\tau}_{1+D}^x | \phi_l \rangle \right) \\ &= L^2 \left(1 + \sum_{D=1}^{L-1} \sum_l \langle l | \rho^{1/2} \hat{\tau}_1^x \hat{\tau}_{1+D}^x \rho^{1/2} | l \rangle \right) \\ &= L^2 \left[1 + \sum_{D=1}^{L-1} \langle l | \hat{\tau}_1^x \hat{\tau}_{1+D}^x \right. \\ &\quad \times \left. \sum_{i=0,1} \prod_i [\tanh(J^A/T) \hat{\tau}_i^x \hat{\tau}_{i+1}^x]^i | l \rangle \right] \\ &= L^2 \left[1 + \sum_{D=1}^{L-1} \tanh(J^A/T)^D \right], \quad (\text{D5}) \end{aligned}$$

where the first index $(2k-1)$ of the dual Pauli operators $\hat{\tau}_{2k-1,j}$ for the original lattice have been omitted, and we have used the fact that $\langle l | \hat{\tau}_{2k-1,j}^x | l \rangle = 0$ and $\langle \phi_l | \hat{\mathcal{O}}^m | \phi_l \rangle = 0$.

Similarly, we consider the QFI with respect to the generator $\hat{\mathcal{O}}^e$. We choose the state $|l'\rangle$ as a product state in the $\hat{\sigma}^x$ basis, and the METTS is written as

$$|\phi_{l'}\rangle = \rho_T^{1/2} |l'\rangle / \sqrt{p_{l'}} \sim \prod_p [1 + \tanh(J^B/(2T)) \hat{B}_p] |l'\rangle, \quad (\text{D6})$$

with $p_{l'} = \langle l' | \rho_T | l' \rangle$. The upper bound of the QFI with respect to the generator $\hat{\mathcal{O}}^e$ [Eq. (6) in the main text] for the METTSs $\{|\phi_{l'}\rangle\}$ can be calculated as

$$F_Q[\hat{\mathcal{O}}^e, \rho_T] \leq \sum_{l'} p_{l'} (\Delta_{\phi_{l'}} \hat{\mathcal{O}}^e)^2 \quad (\text{D7})$$

$$= L^2 \left[1 + \sum_{D=1}^{L-1} \tanh(J^B/T)^D \right]. \quad (\text{D8})$$

- [1] B. Zeng, X. Chen, D.-L. Zhou, and X.-G. Wen, *Quantum Information Meets Quantum Matter: From Quantum Entanglement to Topological Phase in Many-Body Systems* (Springer-Verlag New York, 2019).
- [2] M. Vojta, Quantum phase transitions, *Rep. Prog. Phys.* **66**, 2069 (2003).
- [3] X.-G. Wen, *Quantum Field Theory of Many-Body Systems: From the Origin of Sound to an Origin of Light and Electrons* (Oxford University Press, 2004).
- [4] L. Amico, R. Fazio, A. Osterloh, and V. Vedral, Entanglement in many-body systems, *Rev. Mod. Phys.* **80**, 517 (2008).
- [5] X.-G. Wen, Colloquium: Zoo of quantum-topological phases of matter, *Rev. Mod. Phys.* **89**, 041004 (2017).
- [6] Z. Liu and R. N. Bhatt, Quantum Entanglement as a Diagnostic of Phase Transitions in Disordered Fractional Quantum Hall Liquids, *Phys. Rev. Lett.* **117**, 206801 (2016).
- [7] W. Zhu and D. N. Sheng, Disorder-Driven Transition in the $\nu = 5/2$ Fractional Quantum Hall Effect, *Phys. Rev. Lett.* **123**, 056804 (2019).
- [8] J. Eisert, M. Cramer, and M. B. Plenio, Colloquium: Area laws for the entanglement entropy, *Rev. Mod. Phys.* **82**, 277 (2010).
- [9] J. Eisert, M. Friesdorf, and C. Gogolin, Quantum many-body systems out of equilibrium, *Nat. Phys.* **11**, 124 (2015).
- [10] C. Gogolin and J. Eisert, Equilibration, thermalisation, and the emergence of statistical mechanics in closed quantum systems, *Rep. Prog. Phys.* **79**, 056001 (2016).
- [11] T. E. Lee, F. Reiter, and N. Moiseyev, Entanglement and Spin Squeezing in Non-Hermitian Phase Transitions, *Phys. Rev. Lett.* **113**, 250401 (2014).
- [12] L. Feng, R. El-Ganainy, and L. Ge, Non-Hermitian photonics based on parity-time symmetry, *Nat. Photonics* **11**, 752 (2017).
- [13] R. El-Ganainy, K. G. Makris, M. Khajavikhan, Z. H. Musslimani, S. Rotter, and D. N. Christodoulides, Non-Hermitian physics and PT symmetry, *Nat. Phys.* **14**, 11 (2018).
- [14] Ş. K. Özdemir, S. Rotter, F. Nori, and L. Yang, Parity-time symmetry and exceptional points in photonics, *Nat. Mater.* **18**, 783 (2019).
- [15] N. Matsumoto, K. Kawabata, Y. Ashida, S. Furukawa, and M. Ueda, Continuous Phase Transition Without Gap Closing in Non-Hermitian Quantum Many-Body Systems, *Phys. Rev. Lett.* **125**, 260601 (2020).
- [16] Y. Ashida, Z. Gong, and M. Ueda, Non-Hermitian physics, *Adv. Phys.* **69**, 249 (2020).
- [17] R. Horodecki, P. Horodecki, M. Horodecki, and K. Horodecki, Quantum entanglement, *Rev. Mod. Phys.* **81**, 865 (2009).
- [18] X. G. Wen and Q. Niu, Ground-state degeneracy of the fractional quantum Hall states in the presence of a random potential and on high-genus Riemann surfaces, *Phys. Rev. B* **41**, 9377 (1990).
- [19] Y. Zhou, K. Kanoda, and T.-K. Ng, Quantum spin liquid states, *Rev. Mod. Phys.* **89**, 025003 (2017).
- [20] H. L. Stormer, D. C. Tsui, and A. C. Gossard, The fractional quantum Hall effect, *Rev. Mod. Phys.* **71**, S298 (1999).
- [21] A. Y. Kitaev, Fault-tolerant quantum computation by anyons, *Ann. Phys.* **303**, 2 (2003).
- [22] C. Nayak, S. H. Simon, A. Stern, M. Freedman, and S. Das Sarma, Non-Abelian anyons and topological quantum computation, *Rev. Mod. Phys.* **80**, 1083 (2008).
- [23] A. Kitaev and J. Preskill, Topological Entanglement Entropy, *Phys. Rev. Lett.* **96**, 110404 (2006).
- [24] M. Levin and X.-G. Wen, Detecting Topological Order in a Ground State Wave Function, *Phys. Rev. Lett.* **96**, 110405 (2006).
- [25] H. Li and F. D. M. Haldane, Entanglement Spectrum as a Generalization of Entanglement Entropy: Identification of Topological Order in Non-Abelian Fractional Quantum Hall Effect States, *Phys. Rev. Lett.* **101**, 010504 (2008).
- [26] S. T. Flammia, A. Hamma, T. L. Hughes, and X.-G. Wen, Topological Entanglement Rényi Entropy and Reduced Density Matrix Structure, *Phys. Rev. Lett.* **103**, 261601 (2009).
- [27] G. B. Halász and A. Hamma, Topological Rényi Entropy After a Quantum Quench, *Phys. Rev. Lett.* **110**, 170605 (2013).
- [28] C. Castelnovo, Negativity and topological order in the toric code, *Phys. Rev. A* **88**, 042319 (2013).
- [29] Y. A. Lee and G. Vidal, Entanglement negativity and topological order, *Phys. Rev. A* **88**, 042318 (2013).
- [30] T. Brydges, A. Elben, P. Jurcevic, B. Vermersch, C. Maier, B. P. Lanyon, P. Zoller, R. Blatt, and C. F. Roos, Probing Rényi entanglement entropy via randomized measurements, *Science* **364**, 260 (2019).
- [31] S. L. Braunstein and C. M. Caves, Statistical Distance and the Geometry of Quantum States, *Phys. Rev. Lett.* **72**, 3439 (1994).
- [32] J. Ma, X. G. Wang, C. P. Sun, and F. Nori, Quantum spin squeezing, *Phys. Rep.* **509**, 89 (2011).
- [33] O. Gühne and G. Tóth, Entanglement detection, *Phys. Rep.* **474**, 1 (2009).
- [34] P. Hauke, M. Heyl, L. Tagliacozzo, and P. Zoller, Measuring multipartite entanglement through dynamic susceptibilities, *Nat. Phys.* **12**, 778 (2016).
- [35] H. Strobel, W. Muessel, D. Linnemann, T. Zibold, D. B. Hume, L. Pezzè, A. Smerzi, and M. K. Oberthaler, Fisher information and entanglement of non-Gaussian spin states, *Science* **345**, 424 (2014).
- [36] L. Pezzè, A. Smerzi, M. K. Oberthaler, R. Schmied, and P. Treutlein, Quantum metrology with nonclassical states of atomic ensembles, *Rev. Mod. Phys.* **90**, 035005 (2018).
- [37] G. Mathew, S. L. L. Silva, A. Jain, A. Mohan, D. T. Adroja, V. G. Sakai, C. V. Tomy, A. Banerjee, R. Goreti, Aswathi V. N., R. Singh, and D. Jaiswal-Nagar, Experimental realization of multipartite entanglement via quantum Fisher information in a uniform antiferromagnetic quantum spin chain, *Phys. Rev. Research* **2**, 043329 (2020).
- [38] R. Costa de Almeida and P. Hauke, From entanglement certification with quench dynamics to multipartite entanglement of interacting fermions, *Phys. Rev. Research* **3**, L032051 (2021).
- [39] L. Pezzè, M. Gabbriellini, L. Lepori, and A. Smerzi, Multipartite Entanglement in Topological Quantum Phases, *Phys. Rev. Lett.* **119**, 250401 (2017).
- [40] Y.-R. Zhang, Y. Zeng, H. Fan, J. Q. You, and F. Nori, Characterization of Topological States Via Dual Multipartite Entanglement, *Phys. Rev. Lett.* **120**, 250501 (2018).
- [41] Z. C. Gu and X.-G. Wen, Tensor-entanglement-filtering renormalization approach and symmetry-protected topological order, *Phys. Rev. B* **80**, 155131 (2009).
- [42] X. Chen, Z. C. Gu, and X.-G. Wen, Classification of gapped symmetric phases in one-dimensional spin systems, *Phys. Rev. B* **83**, 035107 (2011).
- [43] A. Kitaev, Anyons in an exactly solved model and beyond, *Ann. Phys.* **321**, 2 (2006).

- [44] G. B. Halász and A. Hama, Probing topological order with Rényi entropy, *Phys. Rev. A* **86**, 062330 (2012).
- [45] K. J. Satzinger, Y.-J. Liu, A. Smith, C. Knapp, M. Newman, C. Jones, Z. Chen, C. Quintana, X. Mi, A. Dunsworth, C. Gidney, I. Aleiner, F. Arute, K. Arya, J. Atalaya, R. Babbush, C. Bardin J., R. Barends, J. Basso, A. Bengtsson *et al.*, Realizing topologically ordered states on a quantum processor, *Science* **374**, 1237 (2021).
- [46] G. Semeghini, H. Levine, A. Keesling, S. Ebadi, T. Wang T., D. Bluvstein, R. Verresen, H. Pichler, M. Kalinowski, R. Samajdar, A. Omran, S. Sachdev, A. Vishwanath, M. Greiner, V. Vuletić, and M. D. Lukin, Probing topological spin liquids on a programmable quantum simulator, *Science* **374**, 1242 (2021).
- [47] V. Giovannetti, S. Lloyd, and L. Maccone, Advances in quantum metrology, *Nat. Photonics* **5**, 222 (2011).
- [48] P. W. Anderson, The resonating valence bond state in La_2CuO_4 and superconductivity, *Science* **235**, 1196 (1987).
- [49] G. Misguich, D. Serban, and V. Pasquier, Quantum Dimer Model on the Kagome Lattice: Solvable Dimer-Liquid and Ising Gauge Theory, *Phys. Rev. Lett.* **89**, 137202 (2002).
- [50] X.-G. Wen, Quantum Orders in an Exact Soluble Model, *Phys. Rev. Lett.* **90**, 016803 (2003).
- [51] Y. Zeng, A. Hama, and H. Fan, Thermalization of topological entropy after a quantum quench, *Phys. Rev. B* **94**, 125104 (2016).
- [52] J. Yu, S.-P. Kou, and X.-G. Wen, Topological quantum phase transition in the transverse Wen-plaquette model, *Europhys. Lett.* **84**, 17004 (2008).
- [53] L. Zhang, S.-P. Kou, and Y. J. Deng, Quench dynamics of the topological quantum phase transition in the Wen-plaquette model, *Phys. Rev. A* **83**, 062113 (2011).
- [54] J. B. Kogut, An introduction to lattice gauge theory and spin systems, *Rev. Mod. Phys.* **51**, 659 (1979).
- [55] E. Fradkin, *Field Theories of Condensed Matter Physics*, 2nd ed. (Cambridge University Press, Cambridge, 2013).
- [56] F. J. Wegner, Duality in generalized Ising models and phase transitions without local order parameters, *J. Math. Phys.* **12**, 2259 (1971).
- [57] L. Pezzè and A. Smerzi, Entanglement, Nonlinear Dynamics, and the Heisenberg Limit, *Phys. Rev. Lett.* **102**, 100401 (2009).
- [58] E. Dennis, A. Kitaev, A. Landahl, and J. Preskill, Topological quantum memory, *J. Math. Phys.* **43**, 4452 (2002).
- [59] A. Kay, Nonequilibrium Reliability of Quantum Memories, *Phys. Rev. Lett.* **102**, 070503 (2009).
- [60] B. J. Brown, D. Loss, J. K. Pachos, C. N. Self, and J. R. Wootton, Quantum memories at finite temperature, *Rev. Mod. Phys.* **88**, 045005 (2016).
- [61] S. Suzuki, J.-I. Inoue, and B. K. Chakrabarti, *Quantum Ising Phases and Transitions in Transverse Ising Models* (Springer, 2012), Vol. 862.
- [62] J. R. Wootton and J. K. Pachos, Bringing Order Through Disorder: Localization of Errors in Topological Quantum Memories, *Phys. Rev. Lett.* **107**, 030503 (2011).
- [63] C. Stark, L. Pollet, A. Imamoğlu, and R. Renner, Localization of Toric Code Defects, *Phys. Rev. Lett.* **107**, 030504 (2011).
- [64] A. Kay, Capabilities of a Perturbed Toric Code as a Quantum Memory, *Phys. Rev. Lett.* **107**, 270502 (2011).
- [65] Y. Zeng, A. Hama, Y.-R. Zhang, J.-P. Cao, H. Fan, and W.-M. Liu, Protecting topological order by dynamical localization, *arXiv:2102.03046* (2021).
- [66] M. B. Hastings and X.-G. Wen, Quasiadiabatic continuation of quantum states: The stability of topological ground-state degeneracy and emergent gauge invariance, *Phys. Rev. B* **72**, 045141 (2005).
- [67] T. J. Osborne, Simulating adiabatic evolution of gapped spin systems, *Phys. Rev. A* **75**, 032321 (2007).
- [68] S. Bravyi, M. B. Hastings, and S. Michalakis, Topological quantum order: Stability under local perturbations, *J. Math. Phys.* **51**, 093512 (2010).
- [69] X. Chen, Z.-C. Gu, and X.-G. Wen, Local unitary transformation, long-range quantum entanglement, wave function renormalization, and topological order, *Phys. Rev. B* **82**, 155138 (2010).
- [70] C. Castelnovo and C. Chamon, Entanglement and topological entropy of the toric code at finite temperature, *Phys. Rev. B* **76**, 184442 (2007).
- [71] O. Hart and C. Castelnovo, Entanglement negativity and sudden death in the toric code at finite temperature, *Phys. Rev. B* **97**, 144410 (2018).
- [72] T.-C. Lu, T. H. Hsieh, and T. Grover, Detecting Topological Order at Finite Temperature Using Entanglement Negativity, *Phys. Rev. Lett.* **125**, 116801 (2020).
- [73] Y.-N. Lu, Y.-R. Zhang, G.-Q. Liu, F. Nori, H. Fan, and X.-Y. Pan, Observing Information Backflow from Controllable Non-Markovian Multichannels in Diamond, *Phys. Rev. Lett.* **124**, 210502 (2020).
- [74] S.-X. Yu, Quantum Fisher information as the convex roof of variance, *arXiv:1302.5311* (2013).
- [75] S. R. White, Minimally Entangled Typical Quantum States at Finite Temperature, *Phys. Rev. Lett.* **102**, 190601 (2009).
- [76] M. Gabbriellini, A. Smerzi, and L. Pezzè, Multipartite entanglement at finite temperature, *Sci. Rep.* **8**, 15663 (2018).
- [77] K. C. Tan, V. Narasimhachar, and B. Regula, Fisher Information Universally Identifies Quantum Resources, *Phys. Rev. Lett.* **127**, 200402 (2021).
- [78] E. Chitambar and G. Gour, Quantum resource theories, *Rev. Mod. Phys.* **91**, 025001 (2019).
- [79] E. Barouch and B. M. McCoy, Statistical mechanics of XY-Model.II. spin-correlation functions, *Phys. Rev. A* **3**, 786 (1971).
- [80] K. Sengupta, S. Powell, and S. Sachdev, Quench dynamics across quantum critical points, *Phys. Rev. A* **69**, 053616 (2004).